Dalton Transactions

Accepted Manuscript

ROYAL SOCIETY OF CHEMISTRY

www.rsc.org/dalton

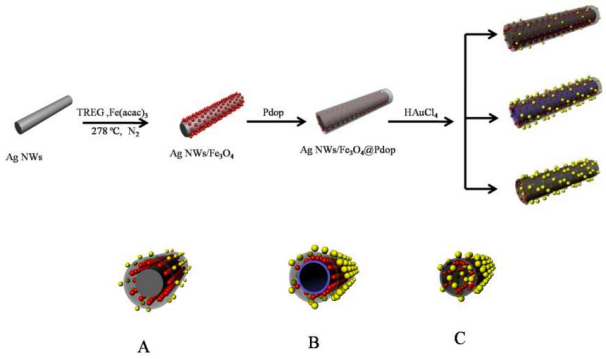

A novel Au(Ag)/AgCl/Fe_3O_4@Pdop@Au multifunctional nanotube was obtained, which showed obvious near-infrared absorption and exhibited excellent photocatalytic *via* visible light.

RSCPublishing

COMMUNICATION

Fabrication of Au(Ag)/AgCl/Fe_3O_4@PDA@Au nanocompositeswith enhanced visible-light-driven photocatalytic activity

Baoyu Wang,Min Zhang,*Weizhen Li,Linlin Wang, Jing Zheng,WenjunGan,*Jingli Xu*

Here we reported a facile method to synthesize multifunctional nanocables with tunable chemical composition. Through the in-situ templating method, the polydopamine could be directly coated onto the magnetic silver nanowires to form Ag NWs/Fe_3O_4@PDA nanocables. Then, the Au(Ag)/AgCl/Fe_3O_4@PDA@Au was elaborately fabricated by utilizing the Ag NWs/Fe_3O_4@PDA as a template by means of spatially confined galvanic replacement and reduction among Ag NWs, PDA and $HAuCl_4$. These multifunctional nanotubes exhibited excellent photocatalytic activity in the presence of visible light.

One dimensional silver nanowires(Ag NWs) have attracted considerable interest due to their intriguing electrical, thermal, and optical properties. [1] Recently, more attention has been paid to functionalize silver nanowires with various inorganic nanoparticles such as metals, metal oxides. [2-6] Among these hybrid Ag NWs, magnetic silver nanowires have been emerging to be an interesting area of advanced research owing to their potential applications in catalysis, polymer reinforcement, and etc.[7]

During the past decade, tremendous research efforts have been devoted to fabricating the large-band gap photocatalysts and improving their absorption coefficient in the visible light region.[8]Among the photocatalysts, plasmonic photocatalysts based on silver halides have attracted much attention because of their excellent photocatalytic performance for dye degradation. [9] For example, AgCl was chosen as a highly efficient and stable photocatalyst due to its large band gap[10]. Furthermore, incorporating noble metal nanostructures(such as Au and Ag nanoparticles) with strong surface plasmon resonance can increase photocatalysts absorption efficiency in the visible light region,[11]because it not only can promote the photocatalytic activity by slowing down the recombination of photogenerated electrons and holes but also can induce a visible-light-driven photocatalysis originating from their plasmonic effects. Up to now, considerable endeavor has been focused on exploring the AgCl-Au as visible-light-responding photocatalyst.[12,13]For instance, Sun group had developed a two-step approach to fabricate AgCl nanowires decorated with Au nanoparticles by using Ag nanowires as chemical templates.[11] Similarly, by using the Fe_3O_4/AgNWs hybrids as the chemical template, Fe_3O_4/Au-AgCl double-layer nanotubes which display obvious near-infrared absorption have also been reported.[14] To our knowledge, the well-defined visible photocatalyst should possess two characteristics, namely near-infrared absorption and excellent photocatalytic stability. Unfortunately, few photocatalysts are present to meet these requirements.

The application of protective shell was an effective strategy for improving the compatibility and stability of the photocatalyst. Polydopamine(PDA)has received significant attention because of its unique chemical structure, outstanding performance and wide potential application.[15] It was reported that the self-polymerization of dopamine could form stable coating on the surface of inorganic and organic materials in comparison to the other coating techniques. [16] Besides its good biocompatibility and adhesiveness, the PDA coatings have other attractive features: serving as a versatile platform for secondary surface-mediated reactions, leading to multifunctional coatings for diverse uses, and so on. [17,18,19] Recently, our group has also extended the application of polydopamine coating on Ag NWs,[20] Fe_3O_4,[21,22] Fe_3O_4@SiO_2,[23] and CNTs/Fe_3O_4[24] through the self-polymerization of dopamine at room temperature. Via this process, PDA can be well deposited on monodisperse ferrite on the outside walls of Ag NWs can be readily obtained. To this end, more involvements should be done to improve the photocatalytic properties by utilizing the PDA chemistry.

Therefore, the novel Au(Ag)/AgCl/Fe_3O_4@PDA@Au multiple layer nanotubes were obtained where in Ag NWs/Fe_3O_4@PDA worked as a template and transformed chemically by means of galvanic replacement and reduction among Ag NWs, PDA and $HAuCl_4$. The design of Au(Ag)/AgCl/Fe_3O_4 hollow structure with PDA-Au coating is one feasible strategy in terms of photocatalytic processes. The advantages of this conception are explained here. First, hollow Au(Ag)/AgCl structure enables both the outer and inner surfaces of the catalyst to contact with the reactants, and allow light scattering of visible light within the interior cavity to promote the light-harvesting efficiency. Second, the incorporation of Au nanoparticles onto the PDA shell can provide them with intriguing stability inherited from the synergetic effect on enhancing the adsorption on the visible light. More importantly, combining the attractive tubular structure with superparamagnetic iron oxide nanoparticles not only has all the advantages of multifunctional nanotubes, but also greatly favors their recycling or targeting abilities by external magnetic field. Consequently, the multifunctional nanocomposites showed obvious near-infrared

absorption and exhibited excellent photocatalytic activity *via* visible light. Here, the Ag NWs/Fe_3O_4@PDA nanocomposites play dual roles. Firstly, the outer layer of PDA can be used as both carrier and reductant to form the PDA-Au composites[25] which can enhance the adorption of the near-infrared light. Secondly, the inner core of Ag NWs serves as chemical template to form the Au(Ag)/AgCl nanotubes, which can also be applied in the photocatalytic reaction.[26,27]

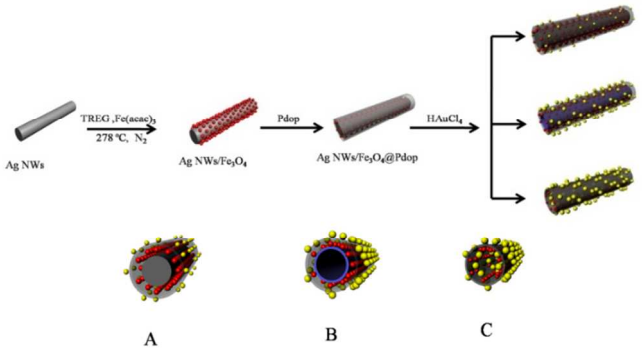

Scheme 1 Programmed synthesis of Au(Ag)/AgCl/Fe_3O_4@PDA@Au by different reaction mass ratio of Ag NWs/Fe_3O_4@PDA to $HAuCl_4$: (A) 7:1, (B) 8:5, (C) 1:7. (Note:The product of A is defined as the Ag(Au)/AgCl/Fe_3O_4@PDA@Au; the product of B is the intermediate product between A and C; The product of C is defined as the Au(Ag)/AgCl/Fe_3O_4@PDA@Au).

Scheme 1 shows the schematic fabrication of the nano-hybrids. Firstly, high-quality AgNWs with length of 4-15 um were synthesized by a facile and scalable one-pot route previously reported [28] (Supporting Information). Secondly, the magnetite nanoparticles were loaded onto the surface of Ag NWs by in-situ high-temperature decomposition of the precursor iron(III) acetylacetonate. [29] The PDA was further coated on the Ag NWs/Fe_3O_4 to improve the functionality of the resultant composites. Finally, Au(Ag)/AgCl/Fe_3O_4@PDA@Au nanocomposites was fabricated by using the Ag NWs/Fe_3O_4@PDA as a chemical template by means of galvanic replacement and reduction among Ag NWs, PDA and $HAuCl_4$.

The standard reduction potential of $AuCl_4^-$/Au pair (0.99 V *vs*. SHE) is higher than that of Ag^+/Ag pair (0.80 V *vs*SHE). Thus the Ag can be oxidized into Ag^+ when the $HAuCl_4$ is added to the suspension of silver nanostructures.[30] Silver nanocrystals/nanowires were usually chosen as the templates for preparing Au nanocages/tubes by means of the galvanic replacement reaction in $HAuCl_4$ aqueous solution [31] and the formed AgCl was removed. Herein, we demonstrate that the Au(Ag)/AgCl/Fe_3O_4@PDA@Au nanocomposites can be prepared based on the galvanic replacement reaction and reduction among Ag NWs, PDA and $HAuCl_4$ under mild environment. Recently, Shim etc[32] have reported the synthesis and characterization of one dimensional Au(Ag)/AgCl nanocomposites. As the Au precursor concentration increased, the structure of the resulting Au(Ag)/AgCl changed from a solid core@shell wire to a porous hollow wire with a decrease in the Ag and AgCl contents and increase in the Au content. Notably, the content of AgCl was decreased with increasing the Au precursor concentration, because the excessive remaining $AuCl_4^-$ can spontaneously dissolve the deposited AgCl into the solution phase by being reduced to Au(Scheme S1).

$$3Ag + HAuCl_4 \longrightarrow Au + 3AgCl + HCl$$

$$AgCl(s) + e^- \longrightarrow Ag(s) + Cl^-$$

Fig. 1A shows X-ray diffraction (XRD) patterns of the Ag NWs, Ag NWs/Fe_3O_4 and PDA coated Ag NWs/Fe_3O_4 nanocomposites. According to the Fig. 1A(a), the XRD pattern of Ag NWs shows broad diffraction peaks at 2θ= 38.2°, 44.5°, 64.4° and 77.5°, which correspond to the (111), (200), (220), and (311) of fcc-silver structure(JCPDS file No. 89-3722), respectively. In the XRD pattern of Ag NWs/Fe_3O_4 composites, two new significant diffraction peaks at 2θ =35.6°, 57.3° are attributed to (311) and (511) planes of Fe_3O_4(JCPDS file No. 19-0629). For the XRD pattern of Ag NWs/Fe_3O_4@PDA(Fig. 1A(c)), the pattern is similar to the pristine Ag NWs/Fe_3O_4 composites(Fig. 1A(a)), revealing that the core-shell composites consist of the Ag NWs/Fe_3O_4 component.

The XRD patterns (Fig.1B) of the as-prepared products of reactions between Ag NWs/Fe_3O_4@PDA and $HAuCl_4$ indicate that the series of nanocomposites are clearly composed of four components, i.e., Ag, AgCl, Fe_3O_4 and Au, where the Ag and Au peaks are almost identical, due to their similar lattice constants. After the oxidation of Ag NWs/Fe_3O_4@PDA nanocomposites by $HAuCl_4$, the as-obtained composites displays different XRD pattern (Fig. 1B) with distinct diffraction peaks of 2θ at 28.2º, 32.6º, 46.6º, 55.2º, 57.8°, 67.6°, which correspond to the (111), (200), (220), (311), (222) and (400) planes of the typical cubic phase of AgCl (JCPDS 31-1238). The compositions of the Ag NWs/Fe_3O_4@PDA with different amount of $HAuCl_4$ are also investigated by XRD(Fig. 1B). Four additional peaks of 2θ at 38.2º, 43º, 64.6º and 77.8º, which represent the Bragg reflections from (111), (200), (200), and (311) planes of Au(JCPDS card No. 04-0784) are observed, showing clearly the existence of Au NPs in the Au(Ag)/AgCl//Fe_3O_4@PDA@Au(Fig. 1B(d)). The XRD result indicates the coexistence of AgCl and Au in the composites nanotubes. It must be mentioned that when the reaction mass ratio of Ag NWs/Fe_3O_4@PDA to $HAuCl_4$ is 1:7, the Ag NWs disappear, which indicates that the inner Ag core is etched to form the Au(Ag)/AgCl hybrids(Fig.1B(d)). The results are consistent with previous work.[32-33] Moreover, the peak intensity of AgCl becomes weaker, this is due to that the excessive $AuCl_4^-$ can spontaneously dissolve the deposited AgCl.[32] Additionally, the diffraction from Fe_3O_4 is too weak to be detected, which is due to the heavy atom effect of Au.[34]

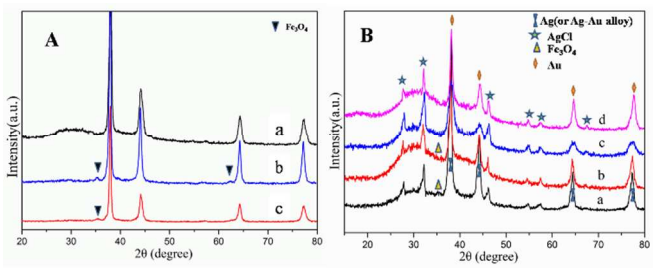

Fig.1 A:XRD patterns of the as-prepared Ag NWs(a), Ag NWs/Fe_3O_4(b) , Ag NWs/Fe_3O_4@PDA(c) **B:**XRD patterns of the as-prepared Ag NWs/Fe_3O_4@PDA with different mass ratios of Ag NWs/Fe_3O_4@PDA to $HAuCl_4$, 7:1(a), 8:5(b), 1:3(c), 1:7(d).

The morphologies of the as-prepared Ag NWs, Ag NWs/Fe_3O_4 and Ag NWs/Fe_3O_4@PDA composites were detected by SEM. Fig. S1(a,b) show SEM photographs of Ag nanowires, indicating that Ag nanowires with smooth surface are of 4-15 umin length and about 100 nm in diameter. Because a layer of tiny Fe_3O_4 nanoparticles is deposited on the surface of Ag nanowires, the resulted Ag NWs/Fe_3O_4 core-shell nanowires display extremely rough surface morphology which are shown in Fig.S1(c,d). Interestingly, after further coating Ag NWs/Fe_3O_4 with a uniform layer of polydopamine, the surface becomes smooth.

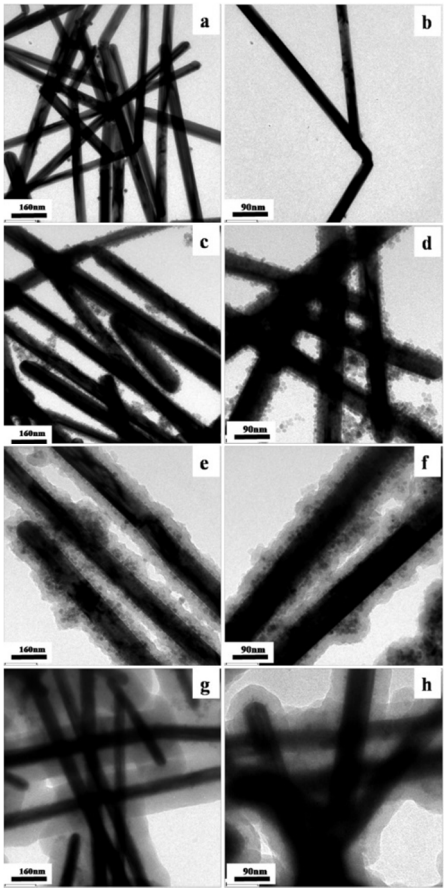

Fig. 2 TEM images of (a,b) Ag NWs, (c,d) Ag NWs/Fe_3O_4 composites, (e,f) Ag NWs/Fe_3O_4@PDA-20 nm,(g,h)Ag NWs/Fe_3O_4@PDA-65 nm.

The microstructure of the as-prepared Ag NWs, Ag NWs/ Fe_3O_4 and Ag NWs/Fe_3O_4@PDA composites were investigated by using TEM. From Fig. 2(c,d), a layer of Fe_3O_4 NPs is found on the Ag NWs(Fig. 2(a,b)). The average diameter of Fe_3O_4 nanoparticles was about 8 nm and they are uniformly distributed on the surface of the Ag NWs. These Ag NWs/Fe_3O_4 composites could be well dispersed into the water solution. Fig. 2(e,f)) were the TEM images of the Ag/Fe_3O_4@PDA, in which we could find that a uniform PDA layer of 15~20 nm is coated on the surface of Ag/Fe_3O_4. The shell thickness is tunable and they can gradually increase from 20 nm to 65 nm (Fig. 2(g,h)) with adjusting the mass ratio of Ag/Fe_3O_4 to dopamine from 1:1 to 1:2. Thus, it can be concluded that coverage thickness can be easily controlled by changing the PDA concentration.

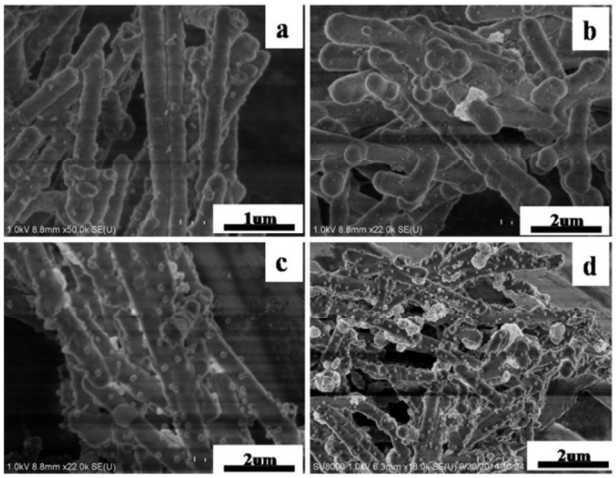

Fig. 3 SEM images of the nanocomposites with increasing the weight ratio between Ag NWs/Fe_3O_4@PDA and $HAuCl_4$: 7:1(a), 8:5(cb), 1:3(c), 1:7(d).

The novel Au(Ag)/AgCl/Fe_3O_4@PDA@Au multiple layer nanotubes were obtained by adding the Ag NWs/Fe_3O_4@PDA to $HAuCl_4$ solution without extra reagents or heat treatment. It is believed that numerous amine and catechol functional groups are present in the PDA coating, and the catechol groups are oxidized. Therefore, the obtained polydopamine shell can act as both reducing agent of metal ions and anchor sites for the resultant metal(0).[15] Furthermore, the impact of $HAuCl_4$ dosage on the size and amount as well as distribution of Au NPs immobilized was investigated. Based on the SEM and TEM analysis, we could find that the size and amount of the Au NPs show strong dependency on the dosage of $HAuCl_4$. From the Fig. 3(a) and Fig. 4(a,b) images,it can be clearly seen that plenty of monodisperse Au NPs with small size were both embedded in PDA shell and distributed on PDA surface. However, with further increasing of the $HAuCl_4$ concentration, the size of AuNPs increased and the excess Au NPs tended to agglomerate to large Au NPs (Fig. 3(b,c,d)).[25] Simultaneously, some ions of silver migrated out of the PDA, and reacted with chloride ion to generate irregular AgCl nanoclusters which were deposited on the surface of PDA.

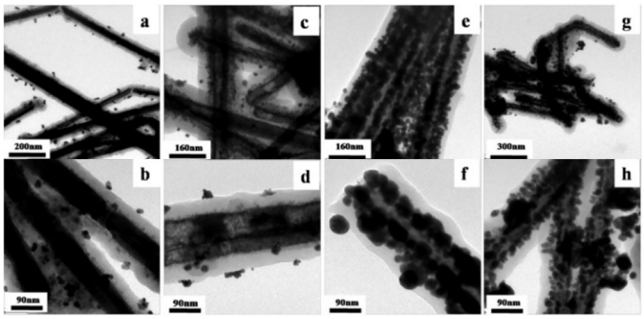

Fig. 4 TEM images of the Ag NWs/Fe_3O_4@PDA@Au composites with increasing the weight ratio between Ag NWs/Fe_3O_4@PDA and $HAuCl_4$ to 7:1(a,b), 8:5(c,d), 1:3(e,f), 1:7(g,h).

TEM images of Fig. 4 show Ag NWs/Fe_3O_4@PDA@Au composites obtained via galvanic displacement reaction between Ag NWs core of the Ag NWs/Fe_3O_4@PDA composites with $HAuCl_4$. During galvanic replacement, the reaction starts at a specific site with the highest surface energy(obvious examples include point defects and stacking faults) of the side {100} surfaces.[35] According to Fig. 4(a,b), it is demonstrated that Ag is oxidized and there are some flaws on the surface of Ag NWs, which is due to the electrons migrating to the entire surface of the nanowire to reduce $AuCl_4^-$ ions into Au atoms. From previous work,[36] it can be concluded that a thin layer of Au nanoparticles are deposited on the surface of AgNWs. As shown in Fig. 4(c,d), the TEM image indicates that with the concentration of $HAuCl_4$ further increasing, the as-obtained nanocomposites display the structure of nanotubes with well-shaped hollow interior and uniform wall. Due to the space occupied by Ag atoms unable to be filled by Au atoms, nanotubes with smooth and uniform wall form composed of Au(Ag)/AgCl composites. Alternatively, if more $HAuCl_4$ reacts with the Au(Ag)/AgCl nanotubes, the remaining $HAuCl_4$ can spontaneously dissolve the deposited AgCl into the solution phase by being reduced to Au. As shown in Fig. 4(e,f), the dealloying process brings about a lot of small pinholes in the Au(Ag)/AgCl nanotube wall. Further dealloying expands the lateral dimensions of the holes and many adjacent ones agglomerate into larger ones. Fragmentation of the porous nanotubes into Au nanoparticles with irregular shapes is triggered by complete (or deep) dealloying (Fig. 4(g,h)). Meanwhile, one-dimensional Au(Ag)/AgCl//Fe_3O_4@PDA@Au nanotubes are obtained through galvanic reaction between Ag/Fe_3O_4 nanowires and $HAuCl_4$. Moreover, it was observed in Fig. S2 that the original Ag nanowires are broken down to several short segments and formation of nanotubes with a uniform, smooth, homogeneous well-shaped hollow interior. Furthermore, the one-dimensional Ag(Au)/AgCl//Fe_3O_4 nanotubes display a different exterior wall from the Ag NWs/Fe_3O_4, which could be attributed to the Ag(Au)/AgCl//Fe_3O_4 nanocomposites.[14] Ag NWs/Fe_3O_4 is easy to be broken apart into small fragments at higher $HAuCl_4$ concentrations without PDA coating; after coated by PDA, the morphology of structures of Ag NWs/Fe_3O_4 reacted with $HAuCl_4$ is kept as before. The experimental results suggest that the PDA coating was aid for the stability of Ag NWs/Fe_3O_4 composites.

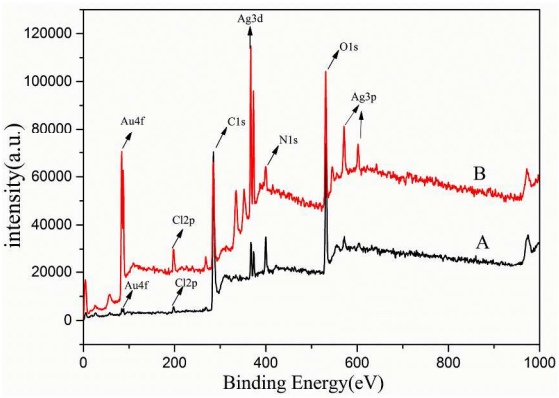

Fig. 5 XPS spectra wide scan of the as-prepared nanocomposites. A: Ag(Au)/AgCl/Fe_3O_4@PDA@Au nanocables (7:1); B: Au(Ag)/AgCl/ Fe_3O_4@PDA@Au(1:7) .

To clarify the elemental and chemical states of the obtained composites, XPS measurement was conducted on the obtained nanocomposites. According to the Fig.5, the XPS spectra from elements of Ag, Cl, C, Au, N and O can be seen. The Cl 2p spectrum in Fig.S4 displays double peaks at 197.5 and 199.1 eV, which could be attributed to the binding energies of Cl $2p_{3/2}$ and Cl $2p_{1/2}$, respectively.[37] The XPS spectrum of Ag 3d could be deconvoluted into two doublets. And the two peaks at 367.4 and 373.4 eV could be attributed to Ag $3d_{3/2}$ and Ag $3d_{5/2}$ of AgCl.9 While, two peaks centered at 84.3 and 88.1 eV could be assigned to Au $4f_{7/2}$ and Au $4f_{5/2}$ (Fig.S3). [25] The spin energy separation of the 4f doublet is 3.8 eV, indicating the metallic nature of gold (Au0). [38] It is worth mentioning that the peak intensity of Cl 2p and Au 4f are greatly improved(Fig. S5), revealing that the surface density of Au nanoparticles and AgCl are greatly improved with increasing the concentration of $HAuCl_4$.

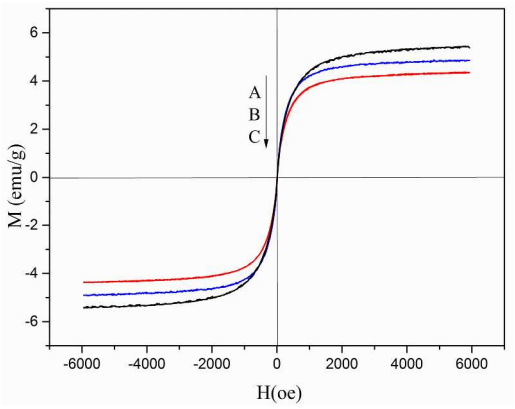

Fig.6 Magnetic hysteresis curves measured at RT of Fe_3O_4/Ag NWs@PDA(A), Ag(Au)-AgCl/Fe_3O_4@PDA@Au nanocables (7:1) (B), and Au(Ag)-AgCl/Fe_3O_4@PDA@Au(1:7) (C).

The magnetic properties of various as-obtained novel nanotubes were evaluated by using the VSM. Fig. 6 shows the M-H hysteresis loops of the nanocomposites measured by sweeping the external field between -0.6 T and 0.6 T at room temperature. The saturation magnetizations of Ag NWs/Fe_3O_4@PDA composites, Ag(Au)/AgCl /Fe_3O_4@PDA@Au nanocables(Ag NWs/Fe_3O_4@PDA composites weight ratio to $HAuCl_4$ = 7:1), Au(Ag)/AgCl/Fe_3O_4@PDA@Au (Ag NWs/Fe_3O_4@PDA composites weight ratio to $HAuCl_4$ =1:7) are approximately 5.4, 4.8, 4.3 emu/g, respectively. Based on these data, we can calculate the mass amount of Fe_3O_4 of composites are about 11.29%(PDA), 9.8%(nanocables), 8.8%(nanotubes). The formula is listed as follows: Fe_3O_4% = (the magnetic saturation values of composites)/(the magnetic saturation values of Fe_3O_4). The VSM value of Fe_3O_4 is shown in Fig. S8. According to the curves we can find that the three samples exhibit superparamagnetic behavior at room temperature with no coercivity and remanence. The saturation magnetization values of Ag(Au)/AgCl/Fe_3O_4@PDA@Au nanocables(7:1) and Au(Ag)/AgCl/Fe_3O_4@PDA@Au(1:7) are lower than Ag NWs/Fe_3O_4@PDA composites (5.4 emu/g) due to the existence of galvanic replacement reaction. However, the relative

magnetization value is enough for efficiently separating the sample from solution with an external magnet.

It has been identified that Au NPs show excellent catalytic activity and selectivity on many catalytic reactions. To evaluate the catalytic activities of the Au NPs decorated on Ag NWs/Fe_3O_4@PDA core-shell nanocomposites, the reduction of methylene blue(MB) in the presence of $NaBH_4$ is chosen as a model reaction system. From the Fig. S6, it can be observed that after adding small amount of Ag(Au)/AgCl/Fe_3O_4@PDA@Au nanocables composites into the mixture of $NaBH_4$ and MB (15 mg/L) , the absorbance at 668， 615 nm successively decreases and nearly disappears at 7 min. The catalytic results reveal that the as-synthesized Ag(Au)/AgCl/Fe_3O_4@PDA@Au nanocables nanocatalyst shows a higher catalytic performance.

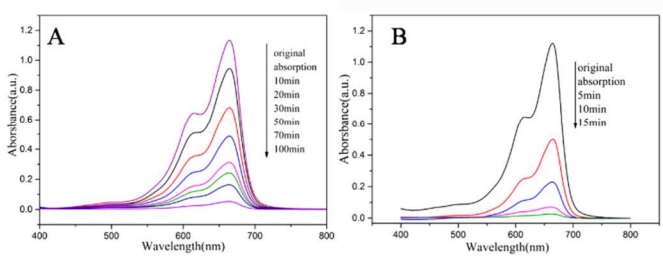

Fig. 7 UV-Vis absorption spectra during the catalytic reduction of methylene blue over nanocomposites composites under visible light. Ag(Au)/AgCl /Fe_3O_4@PDA@Au nanocables (7:1) (A), Au(Ag)/AgCl/Fe_3O_4@PDA@Au(1:7) (B).

Photocatalysts have attracted tremendous research interest in many years because of their unique applications in the degradation of organic pollutants.[39-43] To evaluate the photo-oxidation capability of the magnetic nanocomposites, we examined the decomposition of organic dyes in solution over the as-obtained sample under visible light irradiation. Firstly, the obtained composites (4 mg) were immersed in 50 mL MB aqueous solution (5 mg/L) uniformly. The above mixture was shaken in the dark for 60 min to reach an adsorption-desorption equilibrium between the photocatalyst and MB molecules. Fig.7A shows the evolution of the absorption of MB with light irradiation time on the Ag(Au)/AgCl/Fe_3O_4@PDA@Au nanocables (7:1). It can be seen that MB is degraded slowly by Ag(Au)/AgCl/Fe_3O_4@PDA@Au nanocables(7:1) under visible light. For comparison, MB is degraded quite efficiently by Au(Ag)/AgCl/Fe_3O_4@PDA@Au (1:7) under visible light and after 20 min of irradiation almost all MB has been decomposed(Fig.7B). A possible theory is proposed as follows: When a semiconductor was integrated with gold nanoparticles, the absorption of visible light can be enlarged and the separation process of the photogenerated electrons and holes can be dramatically accelerated.[44] In simple terms, the gold nanoparticles conduce to improvement of the AgCl photocatalytic performance. In addition, from the adsorption equilibrium curves, we can find that the samples in our experiment show very different adsorption ability on MB after 60 minute treatment in the dark. The results is due to that Au(Ag)/AgCl/Fe_3O_4@PDA@Au (1:7) holds more BET surface than that of the Ag(Au)/AgCl/Fe_3O_4@PDA@Au nanocables(7:1). Moreover, after five-cycle tests of MB photodecomposition, there is no significant decrease of photocatalytic activity of the catalyst, indicating the excellent photocatalytic stability of the as-obtained hybrid nanotubes (Fig. S7).

Conclusions

In conclusion, we reported a facile method to prepare well-defined Au(Ag)/AgCl/Fe_3O_4@PDA@Au through galvanic replacement at room temperature. The synthesized nanocomposites show higher catalytic activity in the reduction of MB *via* visible light. More importantly, the outer gold nanoparticles deposited on the surface of the PDA layer play an important role for enhancing optical absorption coefficient of the inner Au(Ag)/AgCl composites in the visible region as well as keeping their stability. Consequently, it is believed that the as-prepared nanocomposites can be used as an efficiency photocatalytic catalyst for practical dye removal treatment. The synthetic method described in this paper could possibly inspire future research in preparation of highly efficient magnetic nanocatalysts for practical catalytic applications.

Acknowledgements

The authors are grateful to the financial support by the National Science Foundation of China (No21305086). The Natural Science Foundation of Shanghai City (13ZR141830), Research Innovation Program of Shanghai Municipal Education Commission (14YZ138),the Special Scientific Foundation for Outstanding Young Teachers in Shanghai Higher Education Institutions (ZZGJD13016), Start-up Funding of Shanghai University of Engineering Science, Shanghai Municipal EducationCommission (Overseas Visiting Scholar Project 20120407), Shanghai Young Teachers' Training-funded Projects(ZZGJD13018), Shanghai University of Engineering ScienceDeveloping founding (grant 2011XZ04), start-up project funding (grant 0501-13-018) and Interdisciplinary Subject Con-struction (grant 2012SCX005).

Note and References

College of Chemistry and Chemical Engineering, ShanghaiUniversity of Engineering Science, Shanghai 201620, China. E-mail: zhangmin@sues.edu.cn;polymer07@sina.com; xujingli@sues.edu.cn.

1 D. Tasis, N. Tagmatarchis, A. Bianco and M. Prato, *Chem.Rev.,* 2006, **106**, 1105.

2 K. Jiang, A. Eitan, L. S. Schadler, P. M. Ajayan, R. W. Siegel, N. Grobert, M. Mayne, M. Reyes-Reyes, H. Terrones and M. Terrones, *Nano Lett,* 2003, **3**, 275.

3 J. Li, S. Tang, L. Lu and H. C. Zeng, *J. Am. Chem. Soc.,* 2007, **129**, 9401.

4 V. D'Anna, D. Duca, F. Ferrante and G. La Manna, *Phys.Chem.Chem.Phys.,* 2009, **11**, 4077.

5 R. Lv, S. Tsuge, X. Gui, K. Takai, F. Kang, T. Enoki, J. Wei, J. Gu, K. Wang and D. Wu, *Carbon,* 2009, **47**, 1141.

6 M. Mazloumi, S. Shadmehr, Y. Rangom, L. F. Nazar and X. Tang, *ACS Nano,* 2013, **7**, 4281.

7 Z. Wang, L. Wu, J. Zhou, W. Cai, B. Shen and Z. Jiang, *J. Phys. Chem. C.,* 2013, **117**, 5446.

8 P.Wang, B.Huang, X. Qin, X. Zhang andY.Dai, *Angew.Chem.Int. Ed.,* 2008, **47**, 7931.

9 L. Sun, R. Zhang, Y .Wang and W.Chen, *ACS Appl .Mater. Inter.,* 2014, **6**, 14819.

10 J. Yu, G. Dai, B. Huang, *J. Phys. Chem. C.,* 2009, **113**, 16394.

11 C. H. An, S. Peng and Y. G. Sun, *Adv.Mater.,* 2010,**22**,2570.

12 J. Yun, S. H. Hwang and J. Jang, Acs*Appl.Mater.Inter.,* 2015, **7**, 2055.

13 A Tanaka, K Fuku, T Nishi, K Hashimoto *J. Phys. Chem. C* 2013, **117**, 16983.

14 Y. Zhai, L. Han, P. Wang, G Li, W. Ren, L. Liu, E .Wang and S. J. Dong, *ACS Nano,* 2011,**5**, 8562.

15 Y. Liu, K. Ai and L. Lu, *Chem Rev,* 2014, **114**, 5057.

16 H. Lee, S. M. Dellatore W. M. Miller , P. B. Messersmith, *Science,* 2007, **318**,426.

17 Y. Mi, Wang, Z. Wang, X. Liu, S. Yang, H. Wang and Z. Wang, *J. Mater. Chem.,* 2012, **22**, 8036.

18 Y. Long, J. Wu, H. Wang, X. Zhang, N. Zhao and J. Xu, *J.Mater. Chem.,* 2011, **21**, 4875.

19 R. Liu, S. M. Mahurin, C. Li, R. R. Unocic, J. C. Idrobo, H. Gao, S. J. Pennycook and S. Dai,*Angew.Chem.Int. Ed.,* 2011, **50**, 6799.

20 M. Zhang, X. Zhang, X. He, L. Chen, and Y. Zhang, *Chem.Lett.*, 2010,**39**, 552.

21 M. Zhang, X. Zhang, X. He, L. Chen, and Y. Zhang, *J. Mater. Chem.,* 2010,**20**, 10696.

22 M. Zhang, X. Zhang, X. He, L. Chen, and Y. Zhang, *Nanoscale*, 2012, **4**, 3141.

23 M. Zhang , J. Zheng, Y. Zheng and J. L. Xu, *RSC Adv.,* 2013,**3**, 13818.

24M. Zhang, X. Zhang, X. He, L. Chen, and Y. Zhang, *J. Mater. Chem.,*2010,**20**, 5835.

25 T.Zeng, H.Niu, Y. Ma, W.Li andY.Cai,*Appl .Catal. B.,* 2013,**134**, 26.

26 J. H. Shim, J. Yang, S. J. Kim, C. Lee and Y. Lee, *J. Mater. Chem. C.,*2012, **22**, 15285.

27 Y. G. Sun, *J. Phys. Chem. C.,* 2010, **114**, 2127.

28 C. Yang, H. W. Gu, W. Lin, M. Matthew, C. P.Wong, M. Y. Xiong, and B.Gao, *Adv. Mater.,*2011, **23**, 3055.

29 B .Wang, M. Zhang, W. Li, L.Wang, J.Zheng and W. Gan,*Dalton Trans.,* 2015,**44**, 7803.

30 Y.Sun, *Nanoscale,* 2010,**2**,1626.

31 J.Yang, D. Shen, L. Zhou, W. Li, X. Li, C. Yao and D. Y. Zhao, *Chem.Mater.,* 2013,**25**, 3030.

32 J. H. Shim, J. Yang, S. J. Kim, C. Lee and Y. Lee, *J. Mater Chem.,* 2012, **22**, 15285.

33 R. Rajendra, P. Bhatia, A. Justin, S. Sharma and N. Ballav, *J .Phys.Chem.C.,* 2015, **119**, 5604.

34 Z .Xu, Y .Hou and S .Sun, *J. Am. Chem. Soc.,* 2007 **129**,8698.

35 Z. L. Wang, T. S. Ahmad and M. A. El-Sayed, *Surf. Sci.,* 1997, **380**,302.

36 S.E. Skrabalak,L.Au, X.Li and Y.Xia, *Nature protocols,* 2007,**2**, 2182.

37 L. Dong, D. Liang, R. Gong, *Eur. J. Inorg. Chem.,* 2012, **19**, 3200.

38 L. Tan, D. Chen, H. Liu and F. Tang, *Adv. Mater.,* 2010, **22**, 4885.

39 Y. Y. Li, Y. Ding, *J.Phys. Chem. C.,*2010, **114**, 3175.

40 C. H. An, R. P. Wang, S. T. Wang, X. Y. Zhang, *J. Mater. Chem.,*2011, **21**, 11532.

41 Z. Z. Lou, B. B. Huang, P. Wang, Z. Y. Wang and X. Y. Qin, *Dalton Trans.,* 2011, **40**, 4104.

42 Y. Li, B. P. Bastakoti, M. Imura and S. M. Hwang, *Chem-Eur. J.,* 2014, **20**, 6027.

43 T. Kimura, Y. Yamauchi and N. Miyamoto,*Chem-Eur. J.,*2011, **17**, 4005.

44 X. Chen, H. Y. Zhu, J. C. Zhao, Z. T. Zheng and X. P. Gao, *Angew. Chem., Int. Ed.,* 2008, **47**, 5353.